

# Cluster-shell competition and effect of adding hyperons

Naoyuki Itagaki<sup>1,2</sup> and Emiko Hiyama<sup>3,4</sup>

<sup>1</sup>*Department of Physics, Osaka Metropolitan University, Osaka 558-8585, Japan*

<sup>2</sup>*Nambu Institute for Theoretical and Experimental Physics,  
Osaka Metropolitan University, Osaka 558-8585, Japan*

<sup>3</sup>*Department of Physics, Graduate School of Science, Tohoku University, Sendai 980-8578, Japan*

<sup>4</sup>*RIKEN Nishina Center for Accelerator-Based Science, Wako 351-0198, Japan*

(Dated: January 6, 2023)

**Background:** The fundamental question is how the hyperon plays a role in the nuclear structure. It is of particular importance, especially in the light mass region, to verify the structure change when  $\Lambda$  particle(s) is added to normal nuclei.

**Purpose:** The ground state of  ${}^8\text{Be}$  has been known to have a well-developed  $\alpha$ - $\alpha$  cluster structure, whereas  ${}^{12}\text{C}$  has a mixed structure of three  $\alpha$  clusters and  $jj$ -coupling shell model, where  $\alpha$  clusters are partially broken. Adding  $\Lambda$  particle(s) could induce the structure change. We compare the Be and C cases.

**Methods:** Using the antisymmetrized quasi-cluster model (AQCM), the  $\alpha$ -cluster states and  $jj$ -coupling shell-model states of  ${}^8\text{Be}$  and  ${}^{12}\text{C}$  are prepared on the same footing, and we add  $\Lambda$  particles. The cluster-shell competition in the ground state can be well described with this model. Using AQCM, we calculate  ${}^8\text{Be}$ ,  ${}^9_\Lambda\text{Be}$ ,  ${}^{10}_{\Lambda\Lambda}\text{Be}$ ,  ${}^{12}\text{C}$ ,  ${}^{13}_\Lambda\text{C}$ , and  ${}^{14}_{\Lambda\Lambda}\text{C}$ .

**Results:** By adding one or two  $\Lambda$  particle(s), the ground state of  ${}^{12}\text{C}$  approaches the  $jj$ -coupling shell model side. On the other hand, in the Be case, although the  $\Lambda$  particle(s) shrinks the  $\alpha$ - $\alpha$  distance, the breaking effect of the cluster structure is rather limited.

**Conclusions:** The spin-orbit interaction is the driving force of breaking the  $\alpha$  clusters, and whether the glue-like effect of  $\Lambda$  particle(s) attracts the cluster inside the range of this interaction is crucial. In  ${}^{14}_{\Lambda\Lambda}\text{C}$ , the breaking of  $\alpha$  clusters in  ${}^{12}\text{C}$  is much enhanced by the addition of the  $\Lambda$  particles than the case of free  ${}^{12}\text{C}$ . We also found that breaking  $\alpha$  clusters in the ground state of  ${}^{14}_{\Lambda\Lambda}\text{C}$  affects the excited state with the pure cluster structure.

## I. INTRODUCTION

One of the most intriguing phenomena of nuclear structure physics is the competition of the shell and cluster structures [1]. This is attributed to the effect of the spin-orbit interaction, which strengthens the symmetry of the  $jj$ -coupling shell model. It is well known that this interaction is vital in explaining the observed magic numbers of 28, 50, 82, and 126 [2]. The spin-orbit interaction also has the effect of breaking clusters [1], where some of the strongly correlated nucleons are spatially localized.

Nevertheless, the  $\alpha$  cluster structure is known to be important in the light mass region. The Be isotopes are known to have the  $\alpha$ - $\alpha$  cluster structure;  ${}^8\text{Be}$  decays into two  $\alpha$  clusters, and the molecular-orbital structure of valence neutrons appears in the neutron-rich Be isotopes [3–5], which is confirmed by the recent *ab initio* shell-model calculation [6]. This persistence of the  $\alpha$ - $\alpha$  cluster structure is owing to the  $\alpha$ - $\alpha$  distance, which is about 3–4 fm and large enough compared with the range of the spin-orbit interaction.

In light nuclei, it is considered that these two different pictures (shell and cluster) coexist, and they compete with each other. Although the  $\alpha$ - $\alpha$  cluster structure may persist in  ${}^8\text{Be}$ , when one more  $\alpha$  cluster is added, in  ${}^{12}\text{C}$ , the interaction among  $\alpha$  clusters gets stronger, and the system has a shorter  $\alpha$ - $\alpha$  distance [7, 8]. In this case, the  $\alpha$  clusters are trapped in the interaction range of the spin-orbit interaction. Although the traditional  $\alpha$  cluster model (Brink model) [9] is incapable of treating

the spin-orbit interaction, its effect is significant if we allow the breaking of the  $\alpha$  clusters. The ground state of  ${}^{12}\text{C}$  is found to have a mixed nature of shell and cluster components [10–12]. On the other hand, the second  $0^+$  state of  ${}^{12}\text{C}$  is well known  $\alpha$  clustering state called the Hoyle state. Since this state is nearby the three- $\alpha$  breakup threshold, the wave function is dilute, and this state has a well-developed  $\alpha$  clustering structure.

It is interesting to investigate how clustering structure is changed when a hyperon such as a  $\Lambda$  particle is injected into  ${}^8\text{Be}$  and  ${}^{12}\text{C}$ . Here it should be noted that there is no Pauli principle between nucleons and a  $\Lambda$ , and the  $\Lambda N$  interaction is attractive, but weaker than  $NN$  interaction. Using this property, some authors studied the structure of  ${}^9_\Lambda\text{Be}$  and  ${}^{13}_\Lambda\text{C}$  from the viewpoint of dynamical change of the core nuclei,  ${}^8\text{Be}$  and  ${}^{12}\text{C}$ , due to the addition of  $\Lambda$  particle. For instance, Motoba *et al.* [13], pointed out that the  $\alpha$ - $\alpha$  distance in  ${}^9_\Lambda\text{Be}$  was shrunk by about 20 % in comparison with that in the  ${}^8\text{Be}$  core nucleus by  $\Lambda$  injection. In the Carbon isotope, one of the present authors (E. H.) pointed out that dynamical change due to the addition of a  $\Lambda$  particle is dependent on the states in the core nucleus of  ${}^{12}\text{C}$  within the framework of  $3\alpha$  and  $3\alpha + \Lambda$  three- and four-body OCM (orthogonal condition model) [14]. The ground state of  ${}^{12}\text{C}$ ,  $0^+_1$ , is a mixture of shell and cluster structure; the  $\alpha$ - $\alpha$  distance does not change due to the addition of a  $\Lambda$  particle. On the other hand, the  $\alpha$ - $\alpha$  distance is dramatically contracted in the Hoyle state of  ${}^{13}_\Lambda\text{C}$ , which is well-developed clustering state [14]. However, it should be noted that

this calculation was done without taking into account the breaking effect of  $\alpha$  clusters in  $^{12}\text{C}$ . In addition, in Ref. [15], they discussed the similarity and difference in several states of  $^{12}\text{C}$  and  $^{13}\text{C}$ . In this way, there are some discussions on the change of the  $\alpha$ - $\alpha$  distance w/o the  $\Lambda$  particle and the change of the structure. However, there remain never discussed effects of the clustering in such Be and C isotopes due to addition of  $\Lambda$  particles. The question is how the clustering is broken when  $\Lambda$  particles shrinks the  $\alpha$ - $\alpha$  distance. The traditional cluster model is incapable of describing such breaking situation and we must extend the model space to incorporate the spin-orbit contribution, which is the driving force of breaking clusters.

Thus, in this work, we focus on how the clustering is changed and broken due to the addition of a  $\Lambda$  particle(s) in  $^8\text{Be}$ ,  $^9_\Lambda\text{Be}$ ,  $^{10}_{\Lambda\Lambda}\text{Be}$ ,  $^{12}\text{C}$ ,  $^{13}_\Lambda\text{C}$ , and  $^{14}_{\Lambda\Lambda}\text{C}$ . In the case of Be isotopes, as mentioned, the  $\Lambda$  particle(s) shrinks the  $\alpha$ - $\alpha$  relative distance [14, 16], but the resultant distance might still be outside the range of the spin-orbit interaction, and the  $\alpha$  cluster structure could persist. On the contrary, when  $\Lambda$  particle(s) is added to  $^{12}\text{C}$ , the distances between clusters get even shorter. Since the spin-orbit interaction works in the inner regions of the nuclear systems, the breaking of  $\alpha$  clusters is expected to be enhanced. Therefore, the ground state would approach more  $jj$ -coupling shell-model side. Indeed, as shown in the study of antisymmetrized molecular dynamics [17], the slightly deformed ground state of  $^{12}\text{C}$  is changed into a spherical shape in  $^{13}_\Lambda\text{C}$ . It is worthwhile to check this point in terms of the cluster-shell competition.

In most of the conventional  $\alpha$  cluster models, the contribution of the non-central interactions (spin-orbit and tensor interactions) vanishes. To include the spin-orbit effect, we have developed the antisymmetrized quasi-cluster model (AQCM) [10, 18–31]. This method allows us to smoothly transform  $\alpha$ -cluster model wave functions to  $jj$ -coupling shell model ones, and we call the clusters that feel the effect of the spin-orbit interaction quasi-clusters. We have previously introduced AQCM to  $^{12}\text{C}$  and discussed the competition between the cluster states and  $jj$ -coupling shell model state [10]. The consistent description of  $^{12}\text{C}$  and  $^{16}\text{O}$ , which has been a long-standing problem of microscopic cluster models, has been achieved. Also, not only the competition between the cluster states and the lowest shell-model configuration, the effect of single-particle excitation was further included in the description of the ground state [30].

This paper is organized as follows. The framework is described in Sec. II. The results are shown in Sec. III. The conclusions are presented in Sec. IV.

## II. FRAMEWORK

The wave function is fully antisymmetrized, and different basis states are superposed based on the generator coordinate method (GCM) after the angular momen-

tum projection, and the amplitude for each basis state is determined by diagonalizing the norm and Hamiltonian matrices.

### A. Single-particle wave function

In our framework, every single particle is described in a Gaussian form as in many traditional cluster models, including the Brink model [9],

$$\phi^{\tau,\sigma}(\mathbf{r}) = \left(\frac{2\nu}{\pi}\right)^{\frac{3}{4}} \exp\left[-\nu(\mathbf{r} - \boldsymbol{\zeta})^2\right] \chi^{\tau,\sigma}, \quad (1)$$

where the Gaussian center parameter  $\boldsymbol{\zeta}$  is related to the expectation value of the position of the nucleon, and  $\chi^{\tau,\sigma}$  is the spin-isospin part of the wave function. The  $\alpha$  cluster is expressed by four nucleons with different spin and isospin sharing the same  $\boldsymbol{\zeta}$  value. For the size parameter  $\nu$ , here we use  $\nu = 1/2b^2$  and  $b = 1.46$  fm. The Slater determinant is constructed from these single-particle wave functions by antisymmetrizing them. The  $\Lambda$  particle is represented by the same local Gaussian-type wave function.

This traditional  $\alpha$  cluster wave function cannot take into account the effect of non-central interactions including the spin-orbit interaction. We can extend the model based on the AQCM, by which the contribution of the spin-orbit interaction due to the breaking of  $\alpha$  clusters is included. Here the  $\boldsymbol{\zeta}$  values in Eq. (1) are changed to complex numbers. When the original value of the Gaussian center parameter  $\boldsymbol{\zeta}$  is  $\mathbf{R}$ , which is real and related to the spatial position of this nucleon, it is transformed by adding the imaginary part as

$$\boldsymbol{\zeta} = \mathbf{R} + i\lambda \mathbf{e}^{\text{spin}} \times \mathbf{R}, \quad (2)$$

where  $\mathbf{e}^{\text{spin}}$  is a unit vector for the intrinsic-spin orientation of this nucleon. The control parameter  $\lambda$  is associated with the breaking of the cluster. After this transformation, the  $\alpha$  clusters are called quasi-clusters. The two nucleons in the same quasi-cluster with opposite spin orientation have  $\boldsymbol{\zeta}$  values that are complex conjugate to each other. This situation corresponds to the time-reversal motion of two nucleons.

In our previous analysis on  $^{12}\text{C}$  [10], we have introduced two parameters representing the distances between quasi-clusters and their breaking ( $\lambda$ ). The subclosure configuration of  $(s_{1/2})^4 (p_{3/2})^8$  of the  $jj$ -coupling shell model can be obtained at the limit of small relative distances and  $\lambda = 1$ .

### B. Angular momentum projection and GCM

Each AQCM Slater determinant is projected to the eigenstates of parity and angular momentum by using

the projection operator  $P_{J^\pi}^K$ ,

$$P_{J^\pi}^K = P^\pi \frac{2J+1}{8\pi^2} \int d\Omega D_{MK}^J R(\Omega). \quad (3)$$

Here  $D_{MK}^J$  is the Wigner  $D$ -function and  $R(\Omega)$  is the rotation operator for the spatial and spin parts of the wave function. This integration over the Euler angle  $\Omega$  is numerically performed. The operator  $P^\pi$  is for the parity projection ( $P^\pi = (1 + P^r)/\sqrt{2}$  for the positive-parity states, where  $P^r$  is the parity-inversion operator), which is also performed numerically.

The AQC basis states with different distances between quasi-clusters and  $\lambda$  values are superposed based on GCM. We also generate Gaussian centers for the  $\Lambda$  particles using random numbers, and the basis states with different positions are superposed. The coefficients  $\{c_i^K\}$  for the linear combination of the Slater determinants are obtained together with the energy eigenvalue  $E$  when we diagonalize the norm and Hamiltonian matrices, namely by solving the Hill-Wheeler equation.

$$\sum_j (\langle \Phi_i | (P_{J^\pi}^K)^\dagger H P_{J^\pi}^K | \Phi_j \rangle - E \langle \Phi_i | (P_{J^\pi}^K)^\dagger P_{J^\pi}^K | \Phi_j \rangle) c_j^K = 0. \quad (4)$$

### C. Hamiltonian

The Hamiltonian consists of kinetic energy and potential energy terms. For the potential part, the interaction consists of the central, spin-orbit, and Coulomb terms. The nucleon-nucleon interaction is Volkov No.2 [32] with the Majorana exchange parameter of  $M = 0.6$ , which has been known to reproduce the scattering phase shift of  ${}^4\text{He}$ - ${}^4\text{He}$  [33]. For the spin-orbit part, we use the spin-orbit term of the G3RS interaction [34], which is a realistic interaction originally developed to reproduce the nucleon-nucleon scattering phase shifts. The strength of the spin-orbit interactions [10] is set to  $V_{ls}^1 = V_{ls}^2 = 1450$  MeV, which reproduces the binding energy of  ${}^{12}\text{C}$  from the three- $\alpha$  threshold. For the nucleon- $\Lambda$  interaction, we employ only the central part; YNG-ND interaction [35]. The  $k_F$  value for  ${}^9_\Lambda\text{Be}$  and  ${}^{10}_{\Lambda\Lambda}\text{Be}$  is  $0.962$  fm $^{-1}$  as in Ref. [14] and  $1.17$  fm $^{-1}$  for  ${}^{13}_\Lambda\text{C}$  and  ${}^{14}_{\Lambda\Lambda}\text{C}$  as in Ref. [17]. For the  $\Lambda$ - $\Lambda$  interaction, we adopt the one called ‘‘NS’’ in Ref. [35], which allows the reproduction of the binding energy of  ${}^6_{\Lambda\Lambda}\text{He}$ .

## III. RESULTS

### A. Ground states of ${}^8\text{Be}$ , ${}^9_\Lambda\text{Be}$ , and ${}^{10}_{\Lambda\Lambda}\text{Be}$

We start the discussion with  ${}^8\text{Be}$ . Our Hamiltonian gives the energy of  $-27.57$  MeV for the  $\alpha$  cluster, and thus,  $-55.1$  MeV is the two- $\alpha$  threshold energy (experimentally  $-56.6$  MeV, to which our theoretical value does

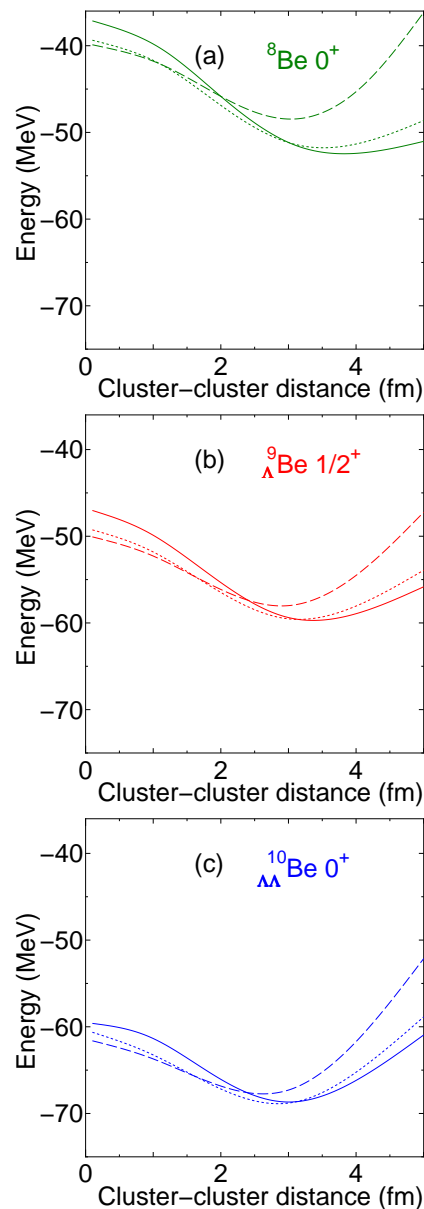


FIG. 1. (a): Energy curves of  $0^+$  state of  ${}^8\text{Be}$  as a function of the distance between two  ${}^4\text{He}$  clusters. Solid line is for  $\lambda = 0$  (pure two  $\alpha$ 's) and dotted and dashed lines are for two quasi-clusters with  $\lambda = 0.1$  and  $0.2$ , respectively. (b): Same as (a) but for the  $1/2^+$  state of  ${}^9_\Lambda\text{Be}$ . (c): Same as (a) but for the  $0^+$  state of  ${}^{10}_{\Lambda\Lambda}\text{Be}$ .

not contradict). Figure 1 (a) shows the energy curves of the  $0^+$  state of  ${}^8\text{Be}$  as a function of the distance between two  ${}^4\text{He}$  clusters. The solid line is for  $\lambda = 0$  (pure two  $\alpha$ 's), and the dotted and dashed line are for two quasi-clusters with  $\lambda = 0.1$  and  $0.2$ , respectively. The energy minimum point appears around the relative distance of  $\sim 3.5$  fm. This distance is quite large, and this is outside of the interaction range of the spin-orbit interaction. Therefore, the  $\lambda$  value that gives the minimum energy is zero (solid line), which means that the  $\alpha$  clusters are

not broken. The  $\alpha$  breaking effect can be seen in more inner regions, where the energies of dotted and dashed lines are lower than the solid line. The  $\alpha$  clusters are surely broken there. However, at short relative distances, the energy itself is high enough, and the spin-orbit interaction only plays a role in reducing the increase of the excitation energy to some extent when two clusters get closer.

The situation is slightly different in Figure 1 (b), which is for the  $1/2^+$  of  ${}^9_{\Lambda}\text{Be}$ , where one  $\Lambda$  particle is added. We superpose 50 Slater determinants with different positions for the  $\Lambda$  particle and diagonalize the Hamiltonian based on the GCM for each cluster-cluster distance and  $\lambda$ . Owing to the  $\Lambda$  particle added, the attractive effect is increased, and the optimal distance between the two  ${}^4\text{He}$  nuclei (lowest energy point) is around 3 fm, slightly shorter than the  ${}^8\text{Be}$  case. Here, the solid line ( $\lambda = 0$ ) and the dotted line ( $\lambda = 0.1$ ) almost degenerate, and thus, the  $\alpha$  clusters are slightly broken due to the spin-orbit effect. The tendency is a bit enhanced in  ${}^{10}_{\Lambda\Lambda}\text{Be}$  shown in Fig 1 (c). The optimal cluster-cluster distance is less than 3 fm, where the dotted line ( $\lambda = 0.1$ ) is slightly lower than the solid line ( $\lambda = 0$ ). The number of Slater determinants with different positions for the  $\Lambda$  particles is increased to 100 for each  ${}^4\text{He}$ - ${}^4\text{He}$  distance and  $\lambda$ . In this way, since the  ${}^4\text{He}$ - ${}^4\text{He}$  distances are large in  ${}^9_{\Lambda}\text{Be}$  and  ${}^{10}_{\Lambda\Lambda}\text{Be}$ , we find that the  $\alpha$ -cluster breaking effect is rather small.

## B. Ground states of ${}^{12}\text{C}$ , ${}^{13}\text{C}$ , and ${}^{14}_{\Lambda\Lambda}\text{C}$

Next we discuss  ${}^{12}\text{C}$  and  ${}^{13}\text{C}$ , and  ${}^{14}_{\Lambda\Lambda}\text{C}$ . The three- $\alpha$  threshold energy is  $-82.7$  MeV in our calculation compared with the experimental value of  $-84.9$  MeV. Figure 2 (a) shows the energy curves of  $0^+$  state of  ${}^{12}\text{C}$  with an equilateral triangular configuration as a function of the distance between two  ${}^4\text{He}$  clusters. The solid line is for  $\lambda = 0$  (pure three  $\alpha$ 's). Since one  ${}^4\text{He}$  is added to  ${}^8\text{Be}$ , the energy minimum point appears around the relative distance of 2.5–3.0 fm, shorter by 1 fm than the previous  ${}^8\text{Be}$  case before allowing the breaking of  $\alpha$  clusters. Therefore, it is considered that the three  $\alpha$  clusters step in the interaction range of the spin-orbit interaction. The dotted line ( $\lambda = 0.1$ ) and dashed line ( $\lambda = 0.2$ ) almost degenerate at the region of the lowest energy (the relative cluster-cluster distance shrinks to 2 fm there).

This tendency is enhanced in Fig. 2 (b), which is for the  $1/2^+$  of  ${}^{13}\text{C}$ , where one  $\Lambda$  particle is added. Owing to the  $\Lambda$  particle added, the attractive effect is increased, and the optimal distance between the  ${}^4\text{He}$  nuclei is around 2.5 fm (solid line) before breaking the  $\alpha$  clusters. When we allow the breaking, the energy curves become almost flat inside the relative  ${}^4\text{He}$ - ${}^4\text{He}$  distance of 2 fm. The energy minimum points of the dotted ( $\lambda = 0.1$ ) and dashed ( $\lambda = 0.2$ ) lines are lower than that of the solid line ( $\lambda = 0$ ).

The attractive effect of the  $\Lambda$  particles is much more en-

hanced in Fig. 2 (c), which is for the  $0^+$  state of  ${}^{14}_{\Lambda\Lambda}\text{C}$ . The optimal distance between the  ${}^4\text{He}$  nuclei (energy minimum point) is around 2.2 fm before breaking the  $\alpha$  clusters (solid line). When we allow the breaking, the energy minimum point appears at the relative cluster-cluster distance of  $\sim 1.4$  fm, where the dashed line ( $\lambda=0.2$ ) gives the lowest energy, and  $\alpha$  clusters are significantly broken. We can confirm that the optimal cluster distance gets shorter, and the breaking of  $\alpha$  clusters becomes larger with the increasing number of  $\Lambda$  particles added to the system.

## C. Superposition of states with different ${}^4\text{He}$ - ${}^4\text{He}$ distance and breaking parameter $\lambda$

To demonstrate the relation between the effect of  $\alpha$  breaking and spin-orbit interaction, we calculate the ground state energies of  ${}^8\text{Be}$ ,  ${}^9_{\Lambda}\text{Be}$ ,  ${}^{10}_{\Lambda\Lambda}\text{Be}$  (Table I) and those of  ${}^{12}\text{C}$ ,  ${}^{13}\text{C}$ ,  ${}^{14}_{\Lambda\Lambda}\text{C}$  (Table II) with two models: ‘‘AQCM’’ which explicitly takes account of the breaking effect of  $\alpha$ , and ‘‘Brink model’’ which does not involve the  $\alpha$  breaking effect ( $\lambda = 0$ ). We superpose Slater determinants with different positions of the  $\Lambda$  particle(s),  ${}^4\text{He}$ - ${}^4\text{He}$  cluster distances, and  $\alpha$ -breaking parameter  $\lambda$  and diagonalize the Hamiltonian based on the GCM.

For the Be case (Table I), the energy difference between Brink and AQCM is less than 0.2 MeV in  ${}^8\text{Be}$ , which means that the spin-orbit interaction does not break the  $\alpha$  clusters since they are separated by a certain distance. The situation is basically the same when  $\Lambda$  particle(s) is added. The difference is about 0.5–0.6 MeV in  ${}^9_{\Lambda}\text{Be}$  and  ${}^{10}_{\Lambda\Lambda}\text{Be}$ . Concerning the ground state energy of  ${}^{10}_{\Lambda\Lambda}\text{Be}$ , the binding energy ( $B_{\Lambda\Lambda}$ ) of  $17.5 \pm 0.4$  MeV from  ${}^8\text{Be}$  has been reported in Ref. [36], which has been revised to  $14.7 \pm 0.4$  MeV in Ref. [37] (see the discussions in Refs. [38, 39]), and the present result (15.23 MeV) is almost consistent with the latter case.

For the C case (Table II), the energy difference between Brink and AQCM is about 3.3 MeV in  ${}^{12}\text{C}$ , and this is much enhanced with the increasing number of the  $\Lambda$  particles added. The difference increases to 5.2 MeV in  ${}^{14}_{\Lambda\Lambda}\text{C}$ . This is because the spin-orbit interaction works in the inner region of the nuclear systems; the glue-like effect of  $\Lambda$  particles shrinks the system and induces more contribution of the spin-orbit interaction.

To clarify the mixing of the  $jj$ -coupling shell model components in each state, we utilize the expectation value of the one-body spin-orbit operator,

$$\hat{O}^{LS} = \sum_i \mathbf{l}_i \cdot \mathbf{s}_i / \hbar^2, \quad (5)$$

where  $\mathbf{l}_i$  and  $\mathbf{s}_i$  are the orbital angular momentum and the spin operators for the  $i$ th nucleon. The sum runs over the nucleons. The expectation value is zero for the pure  $\alpha$  cluster state owing to the antisymmetrization effect. Also, the  $\mathbf{l}_i \cdot \mathbf{s}_i / \hbar^2$  value is 0.5 for one nucleon in the  $p_{3/2}$

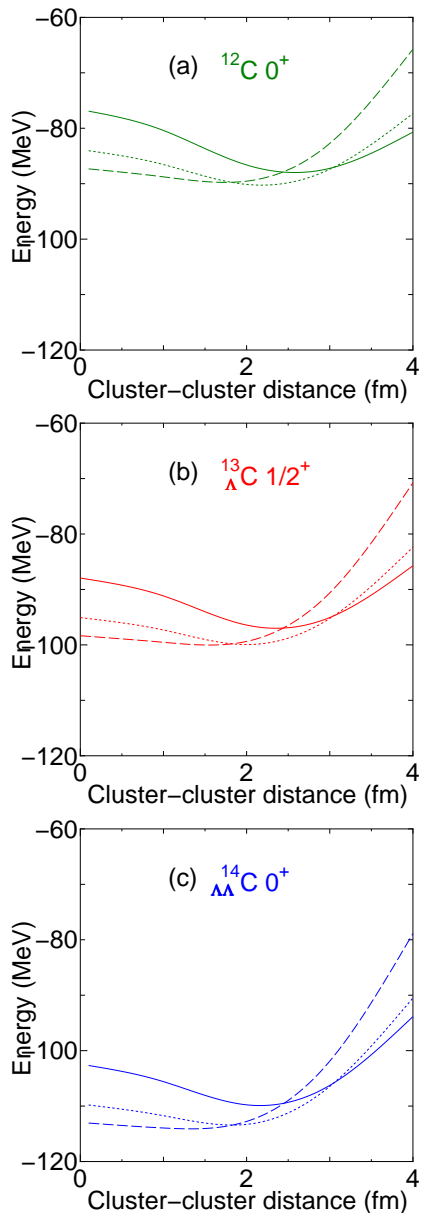


FIG. 2. (a): Energy curves of  $0^+$  state of  $^{12}\text{C}$  as a function of the distance between three  $^4\text{He}$  clusters with equilateral triangular configuration. Solid line is for  $\lambda = 0$  (pure three  $\alpha$ 's) and dotted and dashed lines are for two quasi-clusters with  $\lambda = 0.1$  and  $0.2$ , respectively. (b): Same as (a) but for the  $1/2^+$  state of  $^{13}\text{C}$ . (c) Same as (a) but for the  $0^+$  state of  $^{14}\text{C}$ .

orbit, and the eigen value is 4 for the subclosure configuration of the  $jj$ -coupling shell model ( $((s_{1/2})^4 (p_{3/2})^8)$  in  $^{12}\text{C}$ .

The expectation values of the one-body spin-orbit operator for the ground states of  $^8\text{Be}$ ,  $^9_\Lambda\text{Be}$ , and  $^{10}_{\Lambda\Lambda}\text{Be}$  are listed in the column “one-body LS” in Table I. Although the value increases with the number of  $\Lambda$  particles added, it is rather small and cluster structure is considered to be not broken. However, this is completely different in

TABLE I. Ground state energies of  $^8\text{Be}$ ,  $^9_\Lambda\text{Be}$ , and  $^{10}_{\Lambda\Lambda}\text{Be}$  (“energy ( $J^\pi$ )”) after performing the GCM calculations. “Brink” is for the Brink model ( $\lambda = 0$ ); two- $\alpha$  clusters without the breaking, and “AQCM” is for the AQCM calculation, where different  $\lambda$  states are mixed. “one-body LS” is for the expectation values of the one-body spin-orbit operator. The values in the parenthesis show the experimental values.  $B_\Lambda$ ,  $B_{\Lambda\Lambda}$  are also shown. All energies are in MeV.

$^8\text{Be}$	energy ( $0^+$ )		one-body LS
Brink	-54.75		0.00
AQCM	-54.94	(-56.50)	0.12
$^9_\Lambda\text{Be}$	energy ( $1/2^+$ )	$B_\Lambda$	one-body LS
Brink	-60.97		0.00
AQCM	-61.53	6.59 (6.71 [17])	0.29
$^{10}_{\Lambda\Lambda}\text{Be}$	energy ( $0^+$ )	$B_{\Lambda\Lambda}$	one-body LS
Brink	-69.60		0.00
AQCM	-70.17	15.23 ( $14.7 \pm 0.4$ [37])	0.44

TABLE II. Ground state energies of  $^{12}\text{C}$ ,  $^{13}_\Lambda\text{C}$ , and  $^{14}_{\Lambda\Lambda}\text{C}$  (“energy ( $J^\pi$ )”) after performing the GCM calculations. “Brink” is for the Brink model ( $\lambda = 0$ ); three- $\alpha$  clusters with equilateral triangular shapes without the breaking, and “AQCM” is for the AQCM calculation, where different  $\lambda$  states are mixed. “one-body LS” is for the expectation values of the one-body spin-orbit operator. The values in the parenthesis show the experimental values. All energies are in MeV.

$^{12}\text{C}$	energy ( $0^+$ )		one-body LS
Brink	-86.84		0.00
AQCM	-90.12	(-92.16)	1.55
$^{13}_\Lambda\text{C}$	energy ( $1/2^+$ )	$B_\Lambda$	one-body LS
Brink	-97.77		0.00
AQCM	-102.00	11.88 (11.69 [17])	1.86
$^{14}_{\Lambda\Lambda}\text{C}$	energy ( $0^+$ )	$B_{\Lambda\Lambda}$	one-body LS
Brink	-110.58		0.00
AQCM	-115.74	25.62	2.05

the C case. The expectation values of the one-body spin-orbit operator for the ground states of  $^{12}\text{C}$ ,  $^{13}_\Lambda\text{C}$ , and  $^{14}_{\Lambda\Lambda}\text{C}$  are listed in the column “one-body LS” in Table II. The value is 1.55 for  $^{12}\text{C}$ , and we can reconfirm that the ground state has mixed configurations of shell and cluster aspects. As the number of the  $\Lambda$  particles added increases, we can see that the ground states approach the  $jj$ -coupling shell model side. The values for  $^{13}_\Lambda\text{C}$  and  $^{14}_{\Lambda\Lambda}\text{C}$  are 1.86 and 2.05, respectively.

#### D. pure $\alpha$ cluster state orthogonal to the ground state

We have discussed that the ground states shift to the  $jj$ -coupling shell model side by adding  $\Lambda$  particles, and the final question is where the “pure” three- $\alpha$  cluster state appears in  $^{14}_{\Lambda\Lambda}\text{C}$ . We can discuss it by preparing the pure three- $\alpha$  cluster states and orthogonalizing them to the ground state. The shift of the ground state to the  $jj$ -coupling shell-model-side after allowing the breaking of  $\alpha$  clusters is found to play a crucial role.

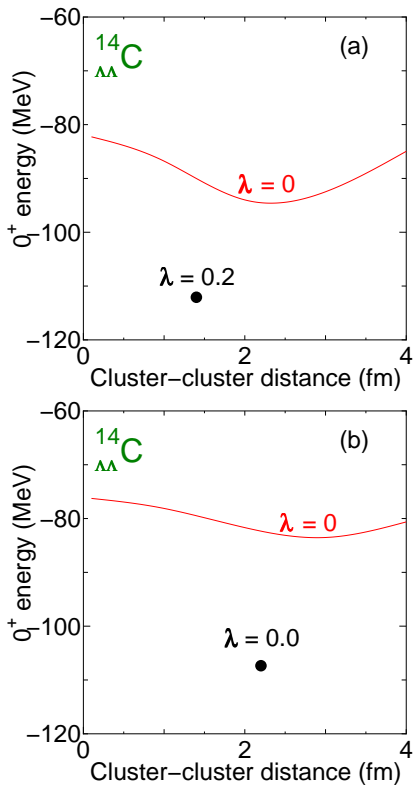


FIG. 3. Excited  $0^+$  state comprised of pure three  $\alpha$  clusters in  $^{14}_{\Lambda\Lambda}\text{C}$  as a function of distances between  $\alpha$ - $\alpha$  (solid lines). Ground state is represented by the AQCM basis state with the  $^4\text{He}$ - $^4\text{He}$  distance of 1.4 fm and  $\lambda = 0.2$  (a) and  $^4\text{He}$ - $^4\text{He}$  distance of 2.2 fm and  $\lambda = 0.0$  (b), which are shown by the solid circles.

The solid line in Fig. 3 (a) shows the excited  $0^+$  state with equilateral triangular configurations of pure three- $\alpha$  clusters as a function of the relative distances between the  $\alpha$  clusters. At each  $\alpha$ - $\alpha$  distance, the wave function is orthogonalized to the ground state. Here the ground state is represented by the optimal AQCM basis state ( $^4\text{He}$ - $^4\text{He}$  distance of 1.4 fm and  $\Lambda = 0.2$ ) shown by the solid circle. Therefore, the two-by-two matrix is diagonalized at every point on the horizontal axis. It is found that the pure cluster state appears around the excitation energy of  $E_x = 15$  MeV with the relative  $\alpha$ - $\alpha$  distance of  $\sim 2.5$  fm. To simplify the discussion, the positions for the Gaussian center parameters for the  $\Lambda$  particles are set to origin only in Figs. 3 (a) and (b).

This situation is quite different if the  $\alpha$  cluster is assumed to be not broken due to the spin-orbit interaction in the ground state. This is an artificial calculation, but we can clearly see the influence of the cluster-shell competition in the excited state; Fig. 3 (b) shows the result when the ground state is represented by the Brink model, which is prepared by changing the  $\lambda$  value to zero and the  $^4\text{He}$ - $^4\text{He}$  distance to 2.2 fm. The excited  $0^+$  state is quite influenced by this change of the ground state. The energy is pushed up by more than 10 MeV, and

the optimal  $\alpha$ - $\alpha$  distance is increased to  $\sim 3$  fm. This is because if the ground state is a pure three- $\alpha$  cluster state, the excited states need to be more clustered to satisfy the orthogonal condition. On the other hand, if the ground state has different components other than the cluster structure, it is easier for the pure cluster state to be orthogonal to the ground state. This effect has been known in  $^{12}\text{C}$  and called the “shrink effect” of the second  $0^+$  state; when the  $\alpha$  breaking component is mixed in the ground state, the second  $0^+$  state orthogonal to the ground state shrinks. We found that this shrinking effect is much more enhanced in  $^{14}_{\Lambda\Lambda}\text{C}$ .

#### IV. CONCLUSIONS

The effect of adding hyperon(s) in nuclear systems is a fundamental problem in nuclear structure physics. We analyzed this effect in the context of cluster-shell competition and discussed the difference between Be and C cases. The antisymmetrized quasi-cluster model (AQCM) is a useful tool to treat the cluster states and shell-model states on the same footing, and we added  $\Lambda$  particle(s) to  $^8\text{Be}$  and  $^{12}\text{C}$ .

The cluster breaking effect is negligibly small in  $^8\text{Be}$ , where  $\alpha$ - $\alpha$  cluster structure keeps enough distance; they stay out of the interaction range of the spin-orbit interaction, which breaks the  $\alpha$  clusters. The situation holds even after  $\Lambda$  particle(s) is added. The glue-like effect of  $\Lambda$  particles surely shrinks the cluster-cluster distance, but clusters are not yet broken.

The situation is completely different in the C case since the additional  $\alpha$  cluster shrinks the cluster-cluster distance, and clusters are in the interaction range of the spin-orbit interaction. The ground state of  $^{12}\text{C}$  contains the component of the  $jj$ -coupling shell model. The energy difference between the traditional Brink model and AQCM is about 3.3 MeV in  $^{12}\text{C}$ , and this is much enhanced with the increasing number of the  $\Lambda$  particles added. The energy difference is about 5.2 MeV in  $^{14}_{\Lambda\Lambda}\text{C}$ . This is because the spin-orbit interaction works in the inner region of the nuclear systems, and the glue-like effect of  $\Lambda$  particles shrinks the system and induces more contribution of the spin-orbit interaction. In  $^{14}_{\Lambda\Lambda}\text{C}$ , the breaking of  $\alpha$  clusters in  $^{12}\text{C}$  is much enhanced by the addition of the  $\Lambda$  particles. The energy and structure of the excited  $0^+$  state with a pure cluster structure are found to be drastically affected by the transition of the ground state to the  $jj$ -coupling shell model side.

#### ACKNOWLEDGMENTS

This work was supported by JSPS KAKENHI Grant Number 19J20543, 22K03618, and JP18H05407. The numerical calculations have been performed using the computer facility of Yukawa Institute for Theoretical Physics, Kyoto University (Yukawa-21).

- 
- [1] N. Itagaki, S. Aoyama, S. Okabe, and K. Ikeda, Cluster-shell competition in light nuclei, *Phys. Rev. C* **70**, 054307 (2004).
- [2] M. G. Mayer and H. G. Jensen, “Elementary theory of nuclear shell structure”, John Wiley, Sons, New York, Chapman, Hall, London (1955).
- [3] N. Itagaki and S. Okabe, Molecular orbital structures in  $^{10}\text{Be}$ , *Phys. Rev. C* **61**, 044306 (2000).
- [4] N. Itagaki, S. Okabe, and K. Ikeda, Important role of the spin-orbit interaction in forming the  $1/2^+$  orbital structure in Be isotopes, *Phys. Rev. C* **62**, 034301 (2000).
- [5] N. Itagaki, S. Hirose, T. Otsuka, S. Okabe, and K. Ikeda, Triaxial deformation in  $^{10}\text{Be}$ , *Phys. Rev. C* **65**, 044302 (2002).
- [6] T. Otsuka, T. Abe, T. Yoshida, Y. Tsunoda, N. Shimizu, N. Itagaki, Y. Utsuno, J. Vary, P. Maris, and H. Ueno,  $\alpha$ -clustering in atomic nuclei from first principles with statistical learning and the hoyle state character, *Nature Communications* **13**, 2234 (2022).
- [7] M. Kamimura, Transition densities between the  $0_1^+$ ,  $2_1^+$ ,  $4_1^+$ ,  $0_2^+$ ,  $2_2^+$ ,  $1_1^-$  and  $3_1^-$  states in  $^{12}\text{C}$  derived from the three-alpha resonating-group wave functions, *Nuclear Physics A* **351**, 456 (1981).
- [8] E. Uegaki, S. Okabe, Y. Abe, and H. Tanaka, Structure of the Excited States in  $^{12}\text{C}$  I, *Prog. Theor. Phys.* **57**, 1262 (1977).
- [9] D. M. Brink, The alpha-particle model of light nuclei, *Proc. Int. School Phys. “Enrico Fermi”* **XXXVI**, 247 (1966).
- [10] N. Itagaki, Consistent description of  $^{12}\text{C}$  and  $^{16}\text{O}$  using a finite-range three-body interaction, *Phys. Rev. C* **94**, 064324 (2016).
- [11] Y. Kanada-En’yo, The Structure of Ground and Excited States of  $^{12}\text{C}$ , *Prog. Theor. Phys.* **117**, 655 (2007).
- [12] M. Chernykh, H. Feldmeier, T. Neff, P. von Neumann-Cosel, and A. Richter, Structure of the Hoyle State in  $^{12}\text{C}$ , *Phys. Rev. Lett.* **98**, 032501 (2007).
- [13] T. Motoba, H. Bando, K. Ikeda, and T. Yamada, Chapter III. Production, Structure and Decay of Light  $p$ -Shell Lambda Hypernuclei, *Progress of Theoretical Physics Supplement* **81**, 42 (1985).
- [14] E. Hiyama, M. Kamimura, T. Motoba, T. Yamada, and Y. Yamamoto, Three- and Four-Body Cluster Models of Hypernuclei Using the G-Matrix  $\Lambda N$  Interaction:  $^9_\Lambda\text{Be}$ ,  $^{13}_\Lambda\text{C}$ ,  $^6_{\Lambda\Lambda}\text{He}$  and  $^{10}_{\Lambda\Lambda}\text{Be}$ , *Progress of Theoretical Physics* **97**, 881 (1997).
- [15] Y. Funaki, M. Isaka, E. Hiyama, T. Yamada, and K. Ikeda, Multi-cluster dynamics in  $^{13}_\Lambda\text{C}$  and analogy to clustering in  $^{12}\text{C}$ , *Physics Letters B* **773**, 336 (2017).
- [16] T. Motoba, H. Bando, and K. Ikeda, Light  $p$ -Shell Hypernuclei by the Microscopic Three-Cluster Model, *Progress of Theoretical Physics* **70**, 189 (1983).
- [17] M. Isaka, M. Kimura, A. Dote, and A. Ohnishi, Deformation of hypernuclei studied with antisymmetrized molecular dynamics, *Phys. Rev. C* **83**, 044323 (2011).
- [18] N. Itagaki, H. Masui, M. Ito, and S. Aoyama, Simplified modeling of cluster-shell competition, *Phys. Rev. C* **71**, 064307 (2005).
- [19] H. Masui and N. Itagaki, Simplified modeling of cluster-shell competition in carbon isotopes, *Phys. Rev. C* **75**, 054309 (2007).
- [20] T. Yoshida, N. Itagaki, and T. Otsuka, Appearance of cluster states in  $^{13}\text{C}$ , *Phys. Rev. C* **79**, 034308 (2009).
- [21] N. Itagaki, J. Cseh, and M. Płoszajczak, Simplified modeling of cluster-shell competition in  $^{20}\text{Ne}$  and  $^{24}\text{Mg}$ , *Phys. Rev. C* **83**, 014302 (2011).
- [22] T. Suhara, N. Itagaki, J. Cseh, and M. Płoszajczak, Novel and simple description for a smooth transition from  $\alpha$ -cluster wave functions to  $jj$ -coupling shell model wave functions, *Phys. Rev. C* **87**, 054334 (2013).
- [23] N. Itagaki, H. Matsuno, and T. Suhara, General transformation of  $\alpha$  cluster model wave function to  $jj$ -coupling shell model in various  $4N$  nuclei, *Prog. Theor. Exp. Phys.* **2016**, 093D01 (2016).
- [24] H. Matsuno, N. Itagaki, T. Ichikawa, Y. Yoshida, and Y. Kanada-En’yo, Effect of  $^{12}\text{C} + \alpha$  clustering on the  $E0$  transition in  $^{16}\text{O}$ , *Prog. Theor. Exp. Phys.* **2017**, 063D01 (2017).
- [25] H. Matsuno and N. Itagaki, Effects of cluster-shell competition and BCS-like pairing in  $^{12}\text{C}$ , *Prog. Theor. Exp. Phys.* **2017**, 123D05 (2017).
- [26] N. Itagaki and A. Tohsaki, Nontrivial origin for the large nuclear radii of dripline oxygen isotopes, *Phys. Rev. C* **97**, 014307 (2018).
- [27] N. Itagaki, H. Matsuno, and A. Tohsaki, Explicit inclusion of the spin-orbit contribution in the Tohsaki-Horiuchi-Schuck-Röpke wave function, *Phys. Rev. C* **98**, 044306 (2018).
- [28] N. Itagaki, A. V. Afanasjev, and D. Ray, Possibility of  $^{14}\text{C}$  cluster as a building block of medium-mass nuclei, *Phys. Rev. C* **101**, 034304 (2020).
- [29] N. Itagaki, T. Fukui, J. Tanaka, and Y. Kikuchi,  $^8\text{He}$  and  $^9\text{Li}$  cluster structures in light nuclei, *Phys. Rev. C* **102**, 024332 (2020).
- [30] N. Itagaki and T. Naito, Consistent description for cluster dynamics and single-particle correlation, *Phys. Rev. C* **103**, 044303 (2021).
- [31] N. Itagaki, T. Naito, and Y. Hirata, Persistence of cluster structure in the ground state of  $^{11}\text{B}$ , *Phys. Rev. C* **105**, 024304 (2022).
- [32] A. Volkov, Equilibrium deformation calculations of the ground state energies of  $1p$  shell nuclei, *Nucl. Phys.* **74**, 33 (1965).
- [33] S. Okabe and Y. Abe, The Structure of  $^9\text{Be}$  by a Molecular Model. II, *Prog. Theor. Phys.* **61**, 1049 (1979).
- [34] R. Tamagaki, Potential Models of Nuclear Forces at Small Distances, *Prog. Theor. Phys.* **39**, 91 (1968).
- [35] Y. Yamamoto, T. Motoba, H. Himeno, K. Ikeda, and S. Nagata, Hyperon-Nucleon and Hyperon-Hyperon Interactions in Nuclei, *Progress of Theoretical Physics Supplement* **117**, 361 (1994).
- [36] M. Danysz, K. Garbowska, J. Pniewski, T. Pniewski, J. Zakrzewski, E. R. Fletcher, J. Lemonne, P. Renard, J. Sacton, W. T. Toner, D. O’Sullivan, T. P. Shah, A. Thompson, P. Allen, M. Heeran, A. Montwill, J. E. Allen, M. J. Beniston, D. H. Davis, D. A. Garbutt, V. A. Bull, R. C. Kumar, and P. V. March, Observation of a double hyperfragment, *Phys. Rev. Lett.* **11**, 29 (1963).
- [37] R. H. Dalitz, D. H. Davis, P. H. Fowler, A. Montwill, J. Pniewski, and J. A. Zakrzewski, The identified  $\Lambda\Lambda$  hypernuclei and the predicted  $H$ -particle, *Proceedings of the Royal Society of London. A. Mathematical and P*

- [38] E. Hiyama, M. Kamimura, T. Motoba, T. Yamada, and Y. Yamamoto, Four-body cluster structure of  $a = 7 - 10$  double- $\Lambda$  hypernuclei, *Phys. Rev. C* **66**, 024007 (2002).
- [39] E. Hiyama and K. Nakazawa, Structure of  $s = -2$  hypernuclei and hyperon-hyperon interactions, *Annual Review of Nuclear and Particle Science* **68**, 131 (2018).